Supplemental Material to the article
"Hall effect anisotropy in the paramagnetic phase of the cage-glass compound $Ho_{0.8}Lu_{0.2}B_{12}$"
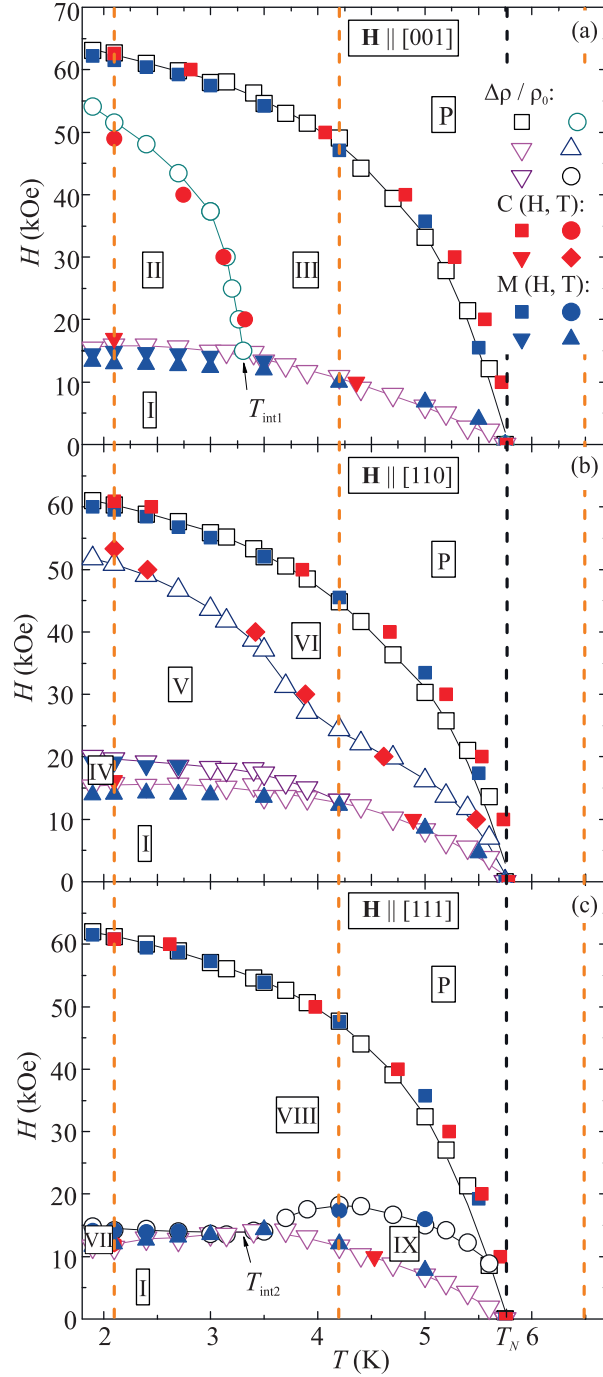

Fig. S1. $H-T$ magnetic phase diagram of $Ho_{0.8}Lu_{0.2}B_{12}$ for magnetic fields applied in the three principal cubic directions in fcc lattice. The phase boundaries are derived from magnetoresistance, heat capacity and magnetization data (see symbols in panel (b)). Roman numerals denote various phases within the antiferromagnetic state. P – paramagnetic phase. Red vertical dotted lines indicate three temperatures ($T = 2.1$, 4.2 and 6.5 K) at which the resistivity and Hall resistance angular dependences have been studied in detail
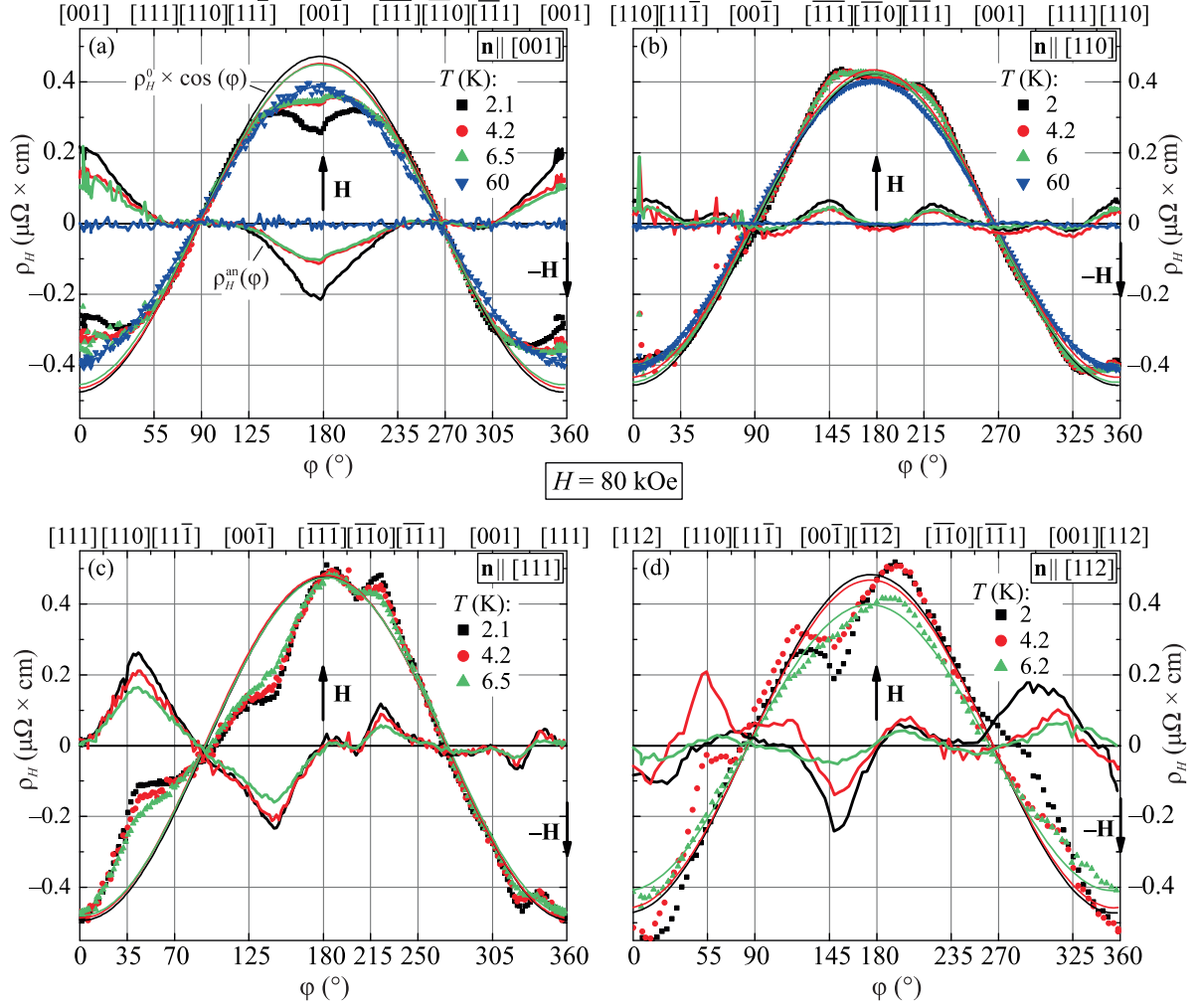
Fig. S2. Angular dependences of the Hall resistivity $\rho_H(\varphi)$ in magnetic field of 80 kOe for the normals $\mathbf{n}\|[001]$, $\mathbf{n}\|[110]$, $\mathbf{n}\|[111]$ and $\mathbf{n}\|[112]$. Thin solid lines show the approximation of the experimental curves by the harmonic dependence $\rho_H^0 \cdot \cos(\varphi)$, thick solid lines show the anharmonic contribution of $\rho_H^{\mathrm{an}}(\varphi)$ to the Hall resistivity (see the text of the paper)
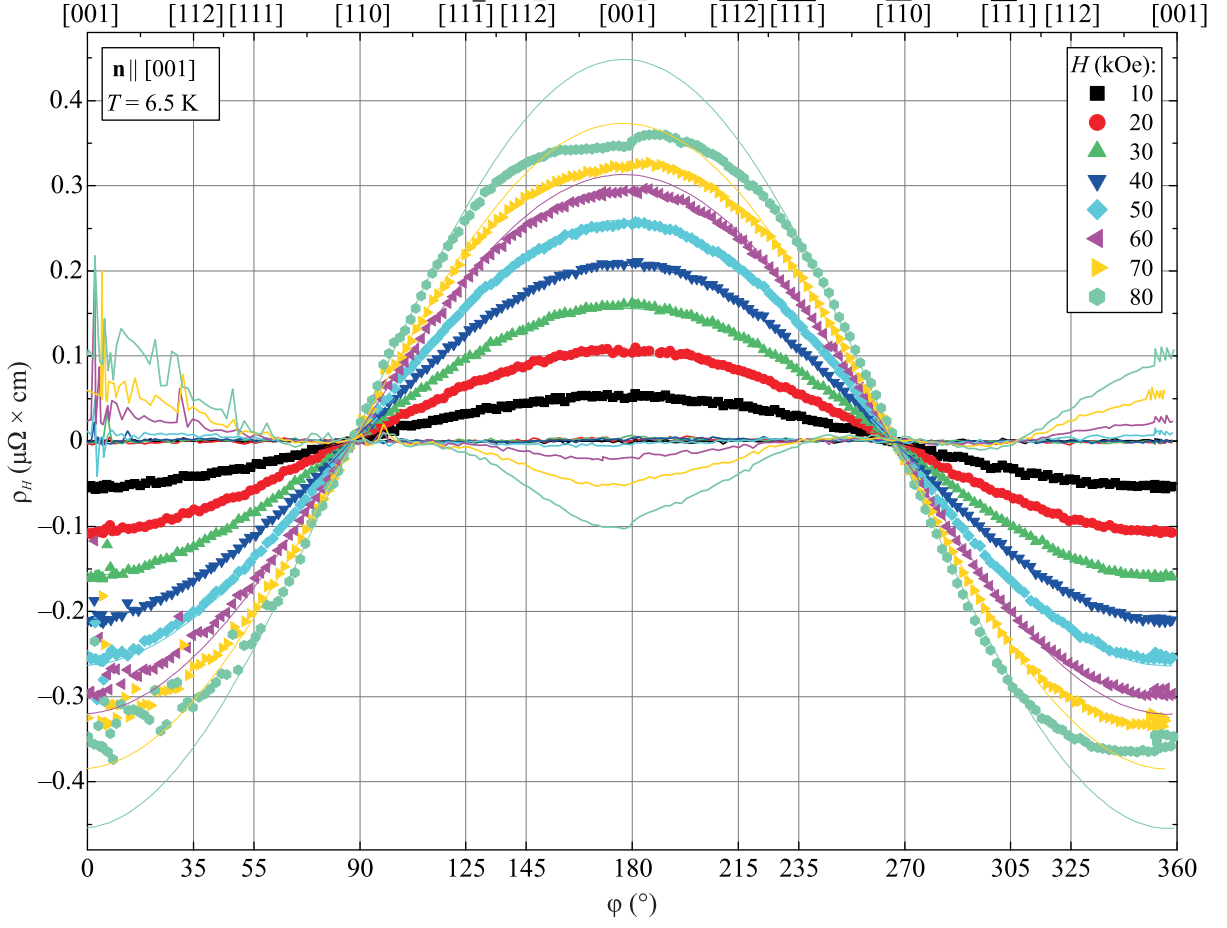
Fig. S3. Angular dependences of the Hall resistivity ρ_H in magnetic fields 10–80 kOe for the normal $\mathbf{n} \| [001]$ at temperature 6.5 K. Thin solid lines show the approximation of the experimental curves by the harmonic dependence $\cos(\varphi)$, thick solid lines show the anharmonic contribution of $\rho_H^{\mathrm{an}}(\varphi)$ to the Hall resistivity (see the text of the paper)
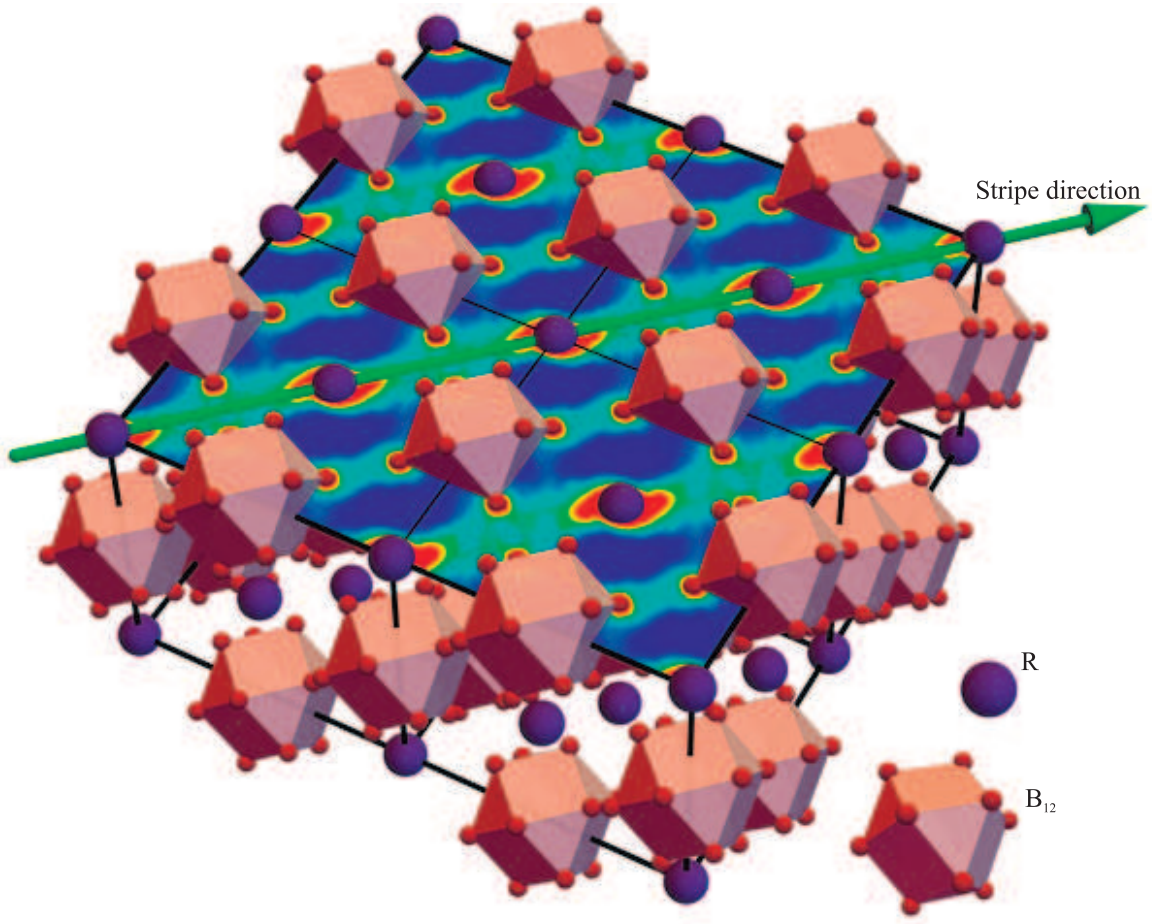
Fig. S4. Crystal structure of the rare-earth dodecaborides RB$_{12}$. Arrow shows the direction $\langle 110 \rangle$, which corresponds to the dynamic charge stripes (shown as wide green lines, see [12, 13, 16] in the paper for more detail)